hydrology

MDPI

Article

Statistical Analysis of the Raindrop Size Distribution Using Disdrometer Data

Evangelos Baltas *, Dimitris Panagos and Maria Mimikou

Department of Water Resources Hydraulic and Maritime Engineering, National Technical University of Athens, 5 Iroon Polytechniou, Athens 15780, Greece; dpanag@chi.civil.ntua.gr (D.P.); mariamimik@chi.civil.ntua.gr (M.M.)

* Correspondence: baltas@chi.civil.ntua.gr; Tel.: +30-2107722883

Academic Editor: Luca Brocca

Received: 13 August 2015; Accepted: 2 February 2016; Published: 19 February 2016

Abstract: The present study utilizes nine years of measurements taken from a Joss–Waldvogel disdrometer (JWD). From this dataset, thirty six rainfall events, were selected and categorized, respectively, in convective and stratiform types, according to specific criteria. Six statistical distributions namely the one- and two-parameter exponential, the two- and three-parameter lognormal and finally the two- and three-parameter gamma were fitted on the observed drop size distributions (DSDs). The goodness-of-fit between each statistical and the observed distribution was determined based on the Kolmogorov–Smirnov test. The results show that 72% of the stratiform events are best described by the three-parameter lognormal distribution while 28% are best described by the three-parameter gamma distribution. In the case of convective events, the results are more diversified; the two- and three-parameter gamma distribution fits best in 39% and 17% of the events, respectively, while the two- and three-parameter lognormal distribution fits best in 6% and 39% of the events. The one- and two-parameter exponential distribution was not the best fit in any case. Moreover, initial steps have already been taken in order for these findings to be used for calibration purposes of a recently employed X-band rainscanner in the Attica region in Greece.

Keywords: Joss–Waldvogel disdrometer; statistical distribution; DSD; rainscanner

1. Introduction

The study of rainfall drop size distribution (DSD) is very useful in a wide spectrum of scientific applications like radar meteorology, microwave communication, satellite remote sensing, soil erosion and cloud physics. There is an increased interest in these areas for several reasons, including climatic change and the consequent increase in the frequency of extreme rainfall phenomena. Accurate measurements of drop size distributions are important for many meteorological applications, including the estimation of rainfall with the use of radar reflectivity measurements, cloud radiative transfer studies and cloud model initialization and verification.

Scientific progress has led to the development of two main types of ground-based disdrometers, for the direct measurement of DSDs; the impact and the optical one. More recently, acoustic disdrometers have been developed, determining rainfall parameters from the produced sound, when a rainfall drop hits a water surface, but their application is still very limited [1]. In optical disdrometers, a source of light (typically laser) and a light detector (e.g., a photodiode) are used to measure the signals that are generated by precipitation particles passing through the measuring area. Several designs of optical disdrometers exist, such as a two-dimensional video disdrometer (2DVD) for *in situ* measurements of precipitation and drop size distribution [2,3].

On the other hand, in impact disdrometers, when rainfall drops hit a solid measuring surface, the mechanical momentum of the impact is transformed into electrical signals. The first automatic impact disdrometer was developed by Joss and Waldvogel [4] and is commonly referred to as the Joss–Waldvogel disdrometer (JWD). The JWD is considered to be a reference instrument for DSD measurements. It has been incorporated in radar-rainfall gauge networks at several ground validation sites across the world. Moreover, among a variety of instruments, it is used for ground validation of the NASA's Global Precipitation Measurement (GPM) mission and many other different field campaigns.

The purpose of this research work is to examine which statistical distribution fits better for the observed size distribution of raindrops N(D). The motivation of this work is the operational calibration of an x-band rainscanner that has recently been deployed in the Attica region for hydrological and flood nowcasting purposes. The statistical distributions that have been selected are the one- and two-parameter exponential (1-P and 2-P exponential), two- and three-parameter gamma (2-P and 3-P gamma) and two- and three-parameter lognormal (2-P and 3-P lognormal) distributions. Many researchers have studied the fit of statistical distributions to DSDs. Ignaccolo and De Michele [5] used the two well-known methods, namely the Method of the Moments and the Method of Maximum Likelihood, to estimate the parameters of the gamma distribution. Then, they tested the adequacy of the gamma distribution through the Kolmogorov–Smirnov goodness-of-fit test, and finally they proposed a different parametrization of the DSD based on some statistical moments. Adirosi *et al.* [6] found that the most of the measured DSD can be described by light-tailed distributions (such as the Weibull or the gamma distribution); however, there is a significant amount of spectra that appears to be better described by a heavy-tailed distribution (such as the lognormal distribution). Furthermore, comparing in pairs only the gamma and the lognormal distribution, they found that the gamma distribution performs better in about 70% of the times.

2. Study Area and Disdrometer Description

The Athens Metropolitan area in the Attica region hosts the capital of Greece and is the most densely populated area of the country. Four large mountains delineate the urban zone of Attica, a densely built up area extending over approximately 430 km^2. The surrounding high mountains and the proximity to the sea affect its meteorological conditions. The climate is typical subtropical Mediterranean, classified as Csa according to the updated world map of the Köppen–Geiger climate classification [7] with prolonged hot and dry summers and considerably mild and wet winters. The mean annual precipitation is approximately 400 mm, with most of the significant rainfall events occurring between September and March, and the mean daily temperature is approximately 27 °C during the summer months and 11 °C during the winter [8].

The hydrometeorological characteristics of the area together with its geomorphological particularities and its land uses contribute significantly to the characterization of the Attica region as a region that is vulnerable to two of the most significant natural hazards, flash floods and forest fires. Thus, the need for regular and accurate monitoring of the hydrometeorological conditions in the area becomes imperative. A monitoring network could support infrastructures for efficient management of floods and a more "human-friendly" design of the urbanized zones [9]. Such a monitoring network is the Hydrological Observatory of Athens (hoa.ntua.gr) that has been developed and maintained by the Hydrology and Water Resources Laboratory of the Civil Engineering School, in National Technical University of Athens (NTUA). The distribution of the stations in the area of Attica is presented in Figure 1. The network is operational since 2005 and consists of 13 meteorological stations and four flow measuring stations, properly located in the greater Athens area. The stations are equipped with sensors that measure environmental parameters of hydrometeorological interest, which include *inter alia*, rainfall, temperature, relative humidity, evaporation, air pressure, solar radiation, sunshine duration, wind direction and velocity. Recently, an x-band rainscanner has also been incorporated into the network that, for the time being, is on calibration stage.

One station of the network is that of "Zografou", which is additionally equipped with the JWD, the records of which are analyzed in the present research work for the proper calibration of the aforementioned rainscanner.

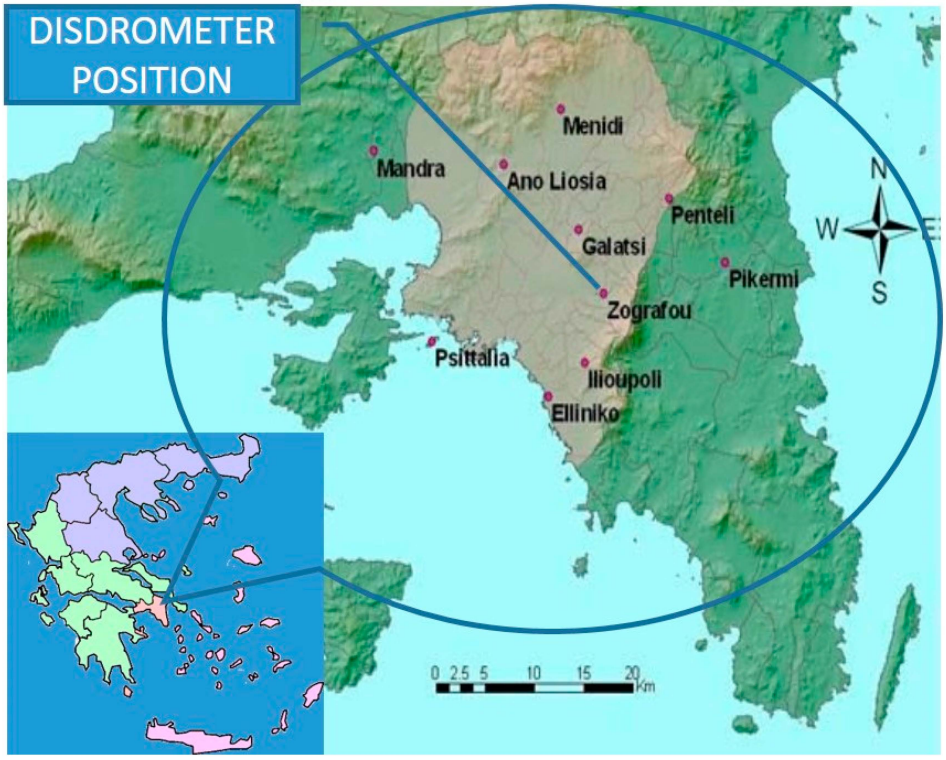

Figure 1. Station locations of the Hydrological Observatory of Athens (HOA).

The JWD was installed at the meteorological station of "Zografou" inside the campus of NTUA and has been operational since November 1997. The data measurements recorded by the JWD, used in this study, span through the time period 2005–2014. Former data could not be utilized because the instrument was installed in a different nearby location. The instrument was uninstalled for approximately two months during the summer due to the temperature sensitivity of the transducer's styrofoam cone.

The JWD consists of three main units [4]: the transducer which is exposed to the rainfall, the processor and the analog to digital converter—the adapter, called Analyzer ADA 90. It is an instrument for measuring raindrop size distributions continuously and automatically. According to the principle of operation, it measures the size distribution of raindrops falling on the sensitive surface of the transducer. The actual drop size distribution in a volume of air may be easily calculated from the measurements. The range of drop diameters that can be measured spans from 0.300 mm to 5.373 mm; drops smaller than 0.300 mm cannot be measured due to practical limits of the measuring principle and are usually of minor importance in applications for which the instrument is intended. Drops larger than 5.373 mm are very rare due to instability of large drops and their breakup. Another shortcoming of the instrument is that it underestimates the number of small drops in heavy rainfall due to the disdrometer's "dead time" [10].

The analog to digital converter ADA-90 is used to analyze the data from the JWD and classifies the diameters of raindrops at 127 channels. To reduce the number of elements and to obtain statistically significant samples, the 127 channels of ADA-90 are combined into 20 diameter categories (bins); each one has a specific diameter range. The number of drops in each category is recorded by the program in frequent time steps (*i.e.*, every minute). While the program 'runs' each time step, a new line appears on the computer screen and gives real time, the number of drops in each diameter category and the rainfall depth during the last minute.

3. Methodology

3.1. Stratiform-Convective Rainfall Classification

Given the considerable size of the data set, a preliminary process has been implemented, in order to aggregate the 1 min measurement samples in discrete rainfall events. Tokay *et al.* [11] reported that the criterion for establishing a new rainfall event was a minimum of a 30-minute rain-free period after the preceding event. In this research, a criterion of 1 h with rainfall accumulation less than 0.2 mm was used. The threshold of 0.2 mm was applied in order to eliminate noise signals that randomly occur. The implementation of this process resulted in 689 rainfall events during the examined period (2005–2014).

Due to the motivation from the study, only rainfall events with considerable accumulation were selected, thus with enhanced probability of resulting in a flash flood, as the operational use of the radar aims mainly in the protection against such events. After consideration, the selection threshold was set at 11.5 mm. This particular threshold does not have a physical meaning rather than a statistical one. It accounts approximately for the upper 10% of rainfall events for the studied period with criterion the total rainfall accumulation.

Moreover, these rainfall events were separated according to their assumed rainfall type. Generally, there are two main mechanisms of precipitation generation; convective and stratiform type. Of course in nature, there are rainfall systems that partially or entirely can not be strictly categorized as of convective or stratiform origin. These mixed type formations are a common case during mesoscale systems [12] where convective cells coexist inside stratiform clouds. As convective rainfall is more capable of producing flash floods, mixed type rainfalls are categorized for the purposes of this work in the convective category due to their convective part, which is a pro-safety assumption.

Convective rainfall or showery precipitation occurs from convective clouds, e.g., cumulonimbus or cumulus congestus. It falls as showers with rapidly changing intensity. Convective precipitation falls over a certain restricted area for a relatively short time, as convective clouds have limited horizontal extent. It is observed mainly from spring to autumn, during the midday and early afternoon, due to the instability of the atmosphere and the relatively high temperatures prevailing until noon. The rainfall in some cases may be accompanied by hail. Such a precipitation is characterized by a considerable amount of higher diameter (>3.0 mm) raindrops.

Stratiform or dynamic precipitation occurs as a consequence of slow ascent of air in large scale systems, such as over surface cold fronts, and over and ahead of warm fronts. This type of rainfall tends to have a long duration and great spatial extent. The frontal rainfall events over the Greek area have maximum frequency in winter. Due to the different rainfall production mechanism, the number of higher diameter (>3.0 mm) droplets is quite less compared with convective events.

Until now, a substantial number of researchers have put effort into classifying rainfall events according to their precipitation type. Tokay and Short [12] have separated stratiform and convective parts of tropical rainfalls using DSDs and more particularly with the fact that when a transition occurs between stratiform and convective rainfall, there is a disproportionate change in No (defined in Equation (1)) in relation with rainfall rate change. It was also noticed that this change is observed around 35–38 dBz, where they defined the threshold of stratiform *vs.* convective rainfall. Bringi *et al.* [13] used a dual polarization C-band radar and the horizontal profiles of clouds in order to separate rainfall events in Darwin, Australia. Caracciolo *et al.* [14] used the ratio of the gamma distribution parameters μ/λ (Equation (3)) to develop a separation algorithm.

In this study, a much simpler criterion was selected for the characterization of the events; events with time duration between 360 and 720 minutes were characterized as stratiform and those with duration shorter than 180 min as convective. This of course does not imply that there is such a clear distinction in practice. The motivation behind this choice is to separate rainfall events based on their flash flood potential. Convective events worldwide, especially in the tropical zone can last for many hours [15]. However, in most cases, in Attica, convective formations do not last for more than three hours, due to their spatially restricted size and increased rainfall intensity. On the other hand,

stratiform rainfall often has a long duration and a sequence of rainfall and no-rainfall intervals is common in the studied area.

By implementation of the first criterion (rainfall accumulation > 11.5 mm), sixty nine rainfall events were isolated by the whole dataset. Furthermore, the implementation of the second criterion has further isolated thirty-six out of the sixty-nine events, eighteen convective and eighteen stratiform. These events are as presented in chronological order in Table 1, where TD is the time duration of the event and RD is the accumulated rainfall depth.

Table 1. Stratiform and convective storm events.

Stratiform				Convective			
No	Rainfall Event	TD(min)	RD(mm)	No	Rainfall Event	TD(min)	RD(mm)
1	24-11-05	536	17.98	1	17-11-05	162	12.05
2	05-01-06	536	40.04	2	05-02-06	136	46.92
3	22-01-06	540	18.78	3	23-09-06	116	13.22
4	07-03-06	440	15.61	4	07-10-06	144	15.84
5	09-10-06	540	58.63	5	19-05-07	158	14.67
6	23-11-06	408	14.94	6	20-10-07	112	13.57
7	11-02-07	622	40.82	7	18-12-08	144	17.94
8	08-12-07	640	29.7	8	21-03-09	142	13.59
9	02-04-08	626	23.04	9	08-02-10	164	13.45
10	27-01-09	376	24.57	10	12-06-11	148	41.12
11	06-04-09	428	12.25	11	21-12-11	176	21.64
12	10-12-09	490	26.66	12	16-01-13	164	33.64
13	28-01-11	496	13.31	13	25-01-13	96	13.71
14	24-02-11	528	11.85	14	11-11-13	58	16.64
15	19-12-11	630	21.33	15	24-11-13	140	14.87
16	18-04-12	376	21.69	16	24-01-14	148	24.81
17	18-05-12	590	16.9	17	26-01-14	140	12.68
18	29-12-12	432	21.09	18	22-02-13	274	63.15

3.2. Statistical Distributions

Various distribution functions have been used by different authors to simulate measured DSDs. In the present study, six common distributions are tested: the 1-P and 2-P exponential, the 2-P and 3-P gamma as well as the 2-P and 3-P lognormal distributions. Additionally to equations found in the literature, the statistical tool "EasyFit 5.6 pro" [16] that was incorporated in the current work for the implementation of the fitting process uses more general equations for each theoretical distribution, which are also presented.

Exponential distribution [17] of the form:

$$N(D) = N_o * e^{(-\lambda D)} \quad (1)$$

where N_0 is the intercept parameter (density of the rainfall drops in the first diameter category of the disdrometer, in which the drop diameter D tends to zero. Units: $mm^{-3} \cdot mm^{-1}$) and

λ is the Slope parameter of the curve N(D) in mm^{-1}.

The statistical tool "EasyFit 5.6 pro" uses the form of Equation (2) for the 2-P exponential distribution:

$$f(x) = \lambda \exp(-\lambda(x - \gamma)) \quad (2)$$

If $\gamma = 0$, then Equation (2) is turned into the 1-P exponential distribution.

Gamma distribution [18] of the form:

$$N(D) = N_o * D^{\mu} * e^{(-\lambda D)} \quad (3)$$

where λ is the slope parameter of the curve N(D) in mm^{-1}, D is the mean diameter for each channel of the disdrometer i = 1, . . . ,20, and μ is the shape parameter of the drop, (when $\mu = 0$, Gamma turns into the Exponential distribution of Equation (1)).

"EasyFit 5.6 pro" uses the generalized form:

$$f(x) = \frac{(x-\gamma)^{\alpha-1}}{\beta^{\alpha}\Gamma(\alpha)}\exp(-(x-\gamma)/\beta) \quad (4)$$

for the 3-P gamma distribution. In this equation, $\Gamma(\alpha)$ is the gamma function. If $\gamma = 0$ then Equation (4) gives the 2-P gamma distribution.

Lognormal distribution [19] of the form:

$$N(D) = \frac{N_T}{\sqrt{2\pi}\ln\sigma D} e^{\left[-\frac{\ln^2(D/D_g)}{2\ln^2\sigma}\right]} \quad (5)$$

where, N_T is the total number of drops per m^3 on the instrument surface, D is the mean diameter for each disdrometer bin i = 1, . . . , 20, D_g is the Geometric mean of the diameter D and σ is the geometric standard deviation of the drop diameter D.

"EasyFit 5.6 pro" for the 3-P lognormal distribution uses the generalized form of Equation (6): (where if $\gamma = 0$ it turns into the 2-P lognormal distribution).

$$f(x) = \frac{\exp\left(-\frac{1}{2}\left(\frac{\ln(x-\gamma)-\mu}{\sigma}\right)^2\right)}{(x-\gamma)\,\sigma\sqrt{2\pi}} \quad (6)$$

For the identification of the goodness-of-fit, the Kolmogorov–Smirnov (K–S) test [5] was applied. As already mentioned, the software tool "EasyFit 5.6 pro" [16] has been used for the fit of the statistical distributions over the observed disdrometer spectra. The mathematical algorithms incorporated in this software for the distribution fit are the Method of Moments (MM), the Maximum Likelihood Method (ML), the least square estimates (LSE), and the method of L-moments (LM). According to the software user's manual, the fitting method for the 1-P exponential distribution as well as the 2-P gamma distribution is the MM, while for the 2-P exponential, the 2-P and 3-P lognormal and the 3-P gamma distributions, is the ML method. The ranking criterion in the K–S test is the estimated test statistic D_n; each D_n is sorted from the smallest to the largest value and the best fit corresponds to the smallest D_n value.

Two points must be mentioned:

(a) This study considers an average DSD during an entire event and not separate DSDs for every minute of spectra measurements. It is known that DSDs vary considerably in time and space during a rainfall event. In addition, an averaged DSD is closer to the exponential distribution than DSDs of smaller time intervals (1–5 min) [6]. Nevertheless, as the scope of this study is the operational calibration of the installed *x*-band rainscanner, it is practically impossible to change the implemented statistical distributions in such detailed time intervals. However, considering whole events instead of 1-min spectra, also had a positive effect in our study; according to Kliche *et al.* [20], as well as, in Cao and Zhang [21], there are discrepancies between various fitting methods like the MM, the ML, and the LM, if are used on the same spectra, unless the sample size is considerable (>1000). In our study, this assumption is valid for all 36 selected events, allowing the results of various fitting methods to be comparable among each other.

(b) The K–S test has two major shortcomings; Firstly, if the parameters of the theoretical distribution (in our case lognormal, gamma and exponential) are estimated by the actual disdrometer data, then there is an overestimation of the test statistic (D_n), and this value must be re-calculated. To overcome this issue, Montecarlo simulations can be implemented [5]. However, as the particular aim of this study is only the relevant ranking of the selected distributions and not the estimation of the exact confidence level and actual test statistic of each distribution, this procedure was considered redundant to this study's aim. Secondly disdrometer data are discrete due to their classification in bins. This presents a limitation of the use of K–S test because it only applies to continuous data. This issue was bypassed by a randomization of the drop diameter in the i-th diameter bin.

4. Results

Initially, a representative curve N(D) for each rainfall type was designed in order to compare the raindrop diameters for the two different rainfall types. For that purpose, the mean value of N(D) for each drop diameter, per rainfall type, was calculated (Figure 2), where a logarithmic scale was used on the vertical axis for the number N of raindrops and decimal scale for the raindrop diameter D in mm, on the horizontal axis. In this Figure, all events per rainfall type are grouped together forming an averaged DSD. The shapes in this Figure justify the applied rainfall type separation methodology due to the fact that, in general, convective events have more raindrops in the higher diameters, in comparison with the stratiform ones—something that is clearly depicted.

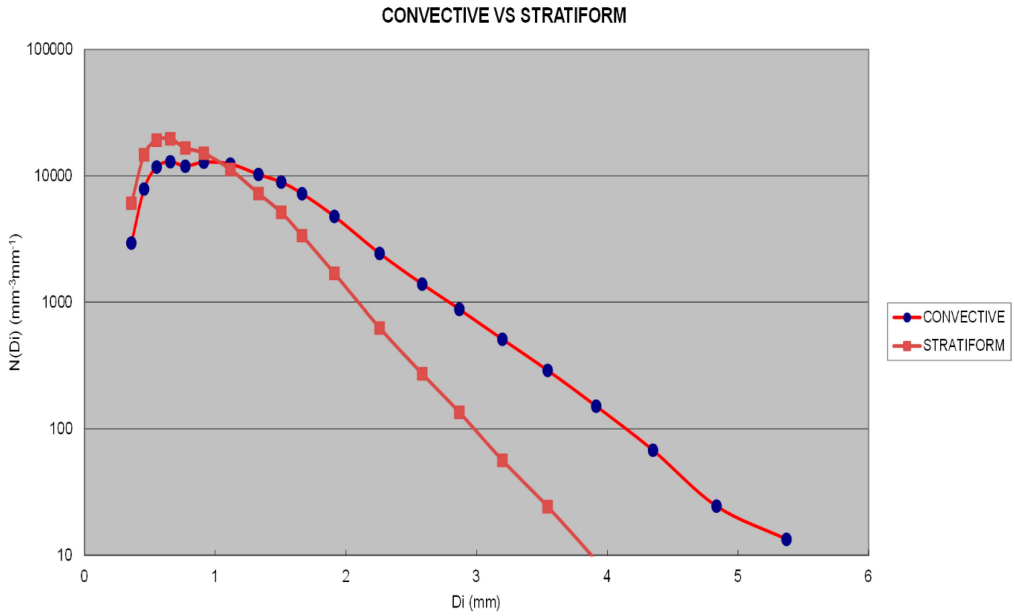

Figure 2. Representative curve N(D) for each rainfall type (convective and stratiform).

Diagrams of N(D) were constructed for each rainfall event. Figure 3 presents the 18 convective, while Figure 4 presents the respective 18 stratiform selected events.

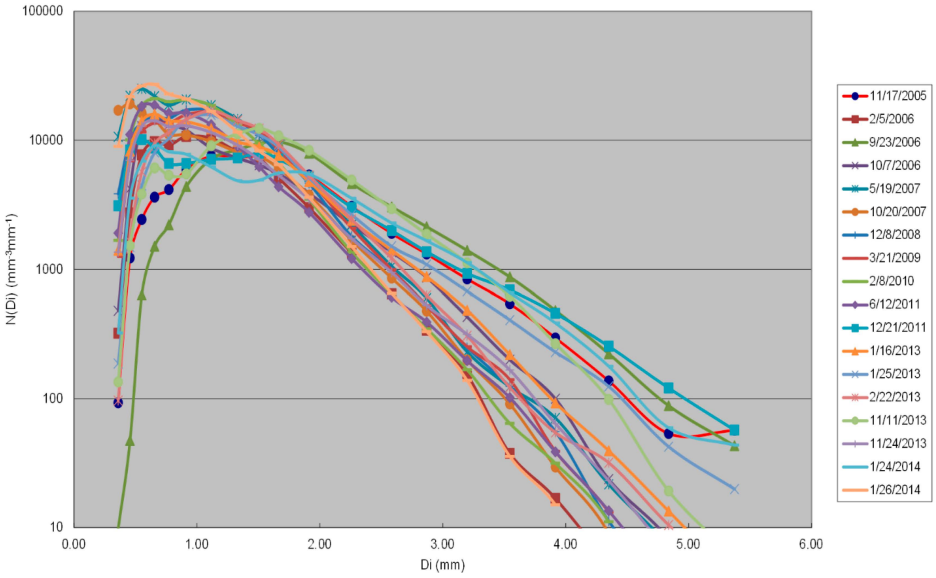

Figure 3. The DSDs of the 18 convective events.

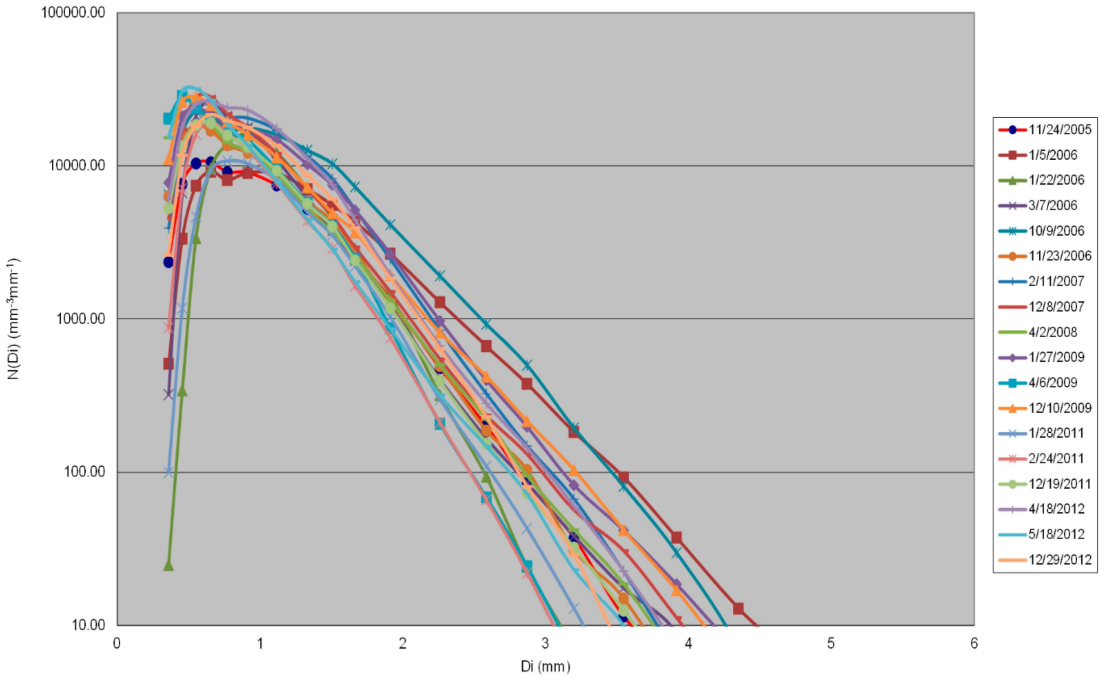

Figure 4. The DSDs of the 18 stratiform events.

In Figures 5–7 the fitting for some statistical distribution expressed in probability density functions (PDFs) is presented for the convective event of 17/11/2005.

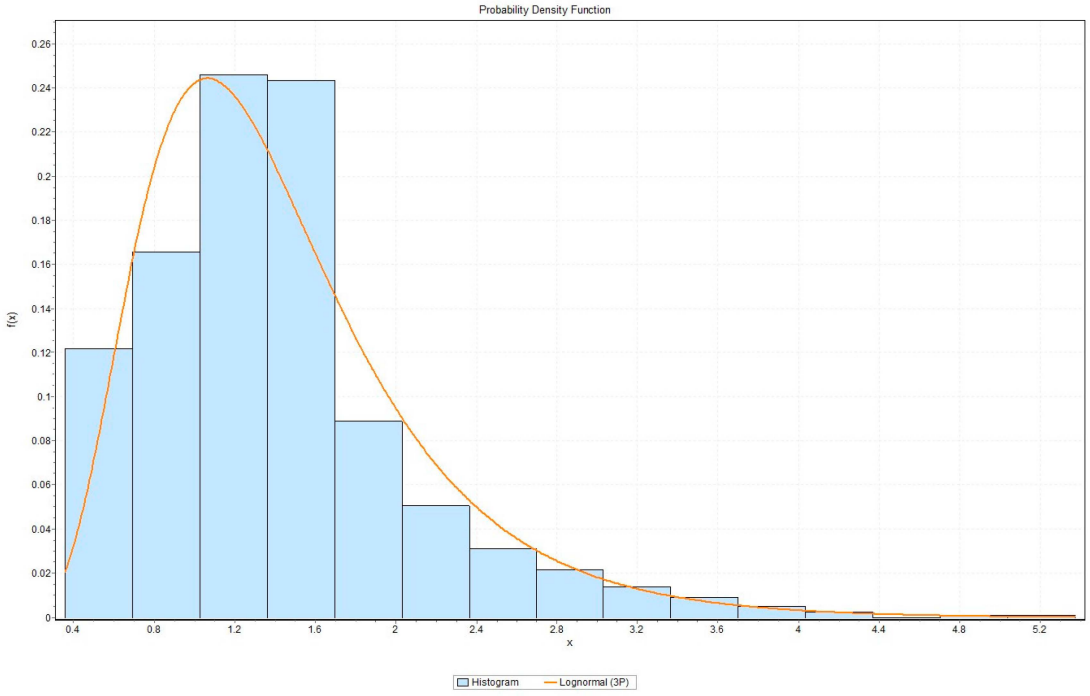

Figure 5. Probability density function for the 3-P lognormal distribution during the event of 17/11/2005.

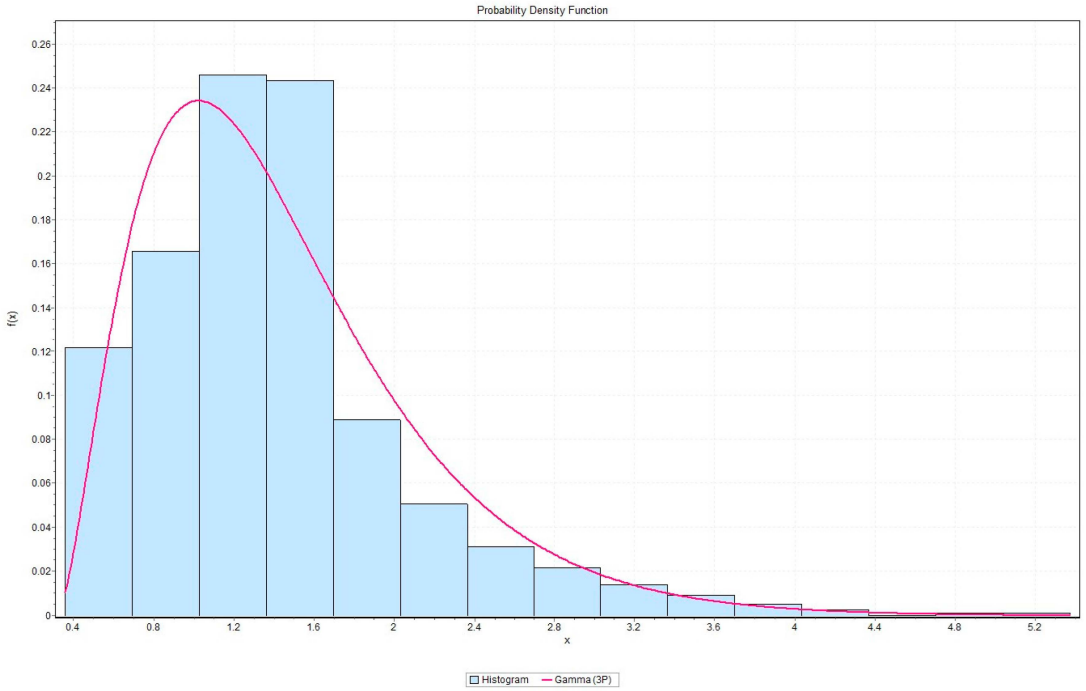

Figure 6. Probability density function for the 3-P gamma distribution during the event of 17/11/2005.

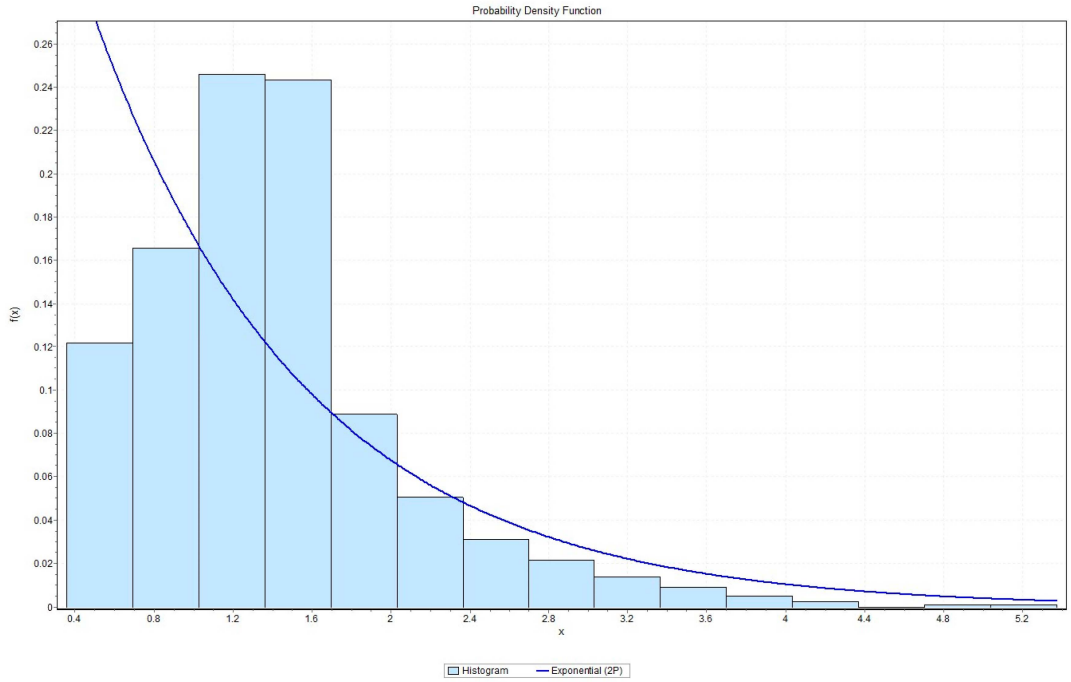

Figure 7. Probability density function for the 2-P exponential distribution during the event of 17/11/2005.

In Table 2, the fitting results of the 17/11/2005 event are presented, using Equations (2), (4) and (6), respectively.

The application of the Kolmogorov–Smirnov test to the selected stratiform and convective events are presented in Tables 3 and 4 respectively. In these Tables, the number under the various distributions denotes the fitting rank according to the lower test statistic D_n. Number 1 is the best fit while number 6 the worst.

Table 2. Fitting results for the event of 17/11/2005.

Fitting Results	Convective Event of 17-11-05	
	Distribution	**Parameters**
1	Exponential (1P)	$\lambda = 0.7468$
2	Exponential (2P)	$\lambda = 0.97022$ $\gamma = 0.30835$
3	Gamma (2P)	$\alpha = 4.2996$ $\beta = 0.31143$
4	Gamma (3P)	$\alpha = 2.7315$ $\beta = 0.38971$ $\gamma = 0.27455$
5	Lognormal (2P)	$\sigma = 0.47132$ $\mu = 0.18308$
6	Lognormal (3P)	$\sigma = 0.44221$ $\mu = 0.24633$ $\gamma = -0.07061$

Table 3. Best fit for stratiform events.

Event Date	Exponential (1P)	Exponential (2P)	Gamma (2P)	Gamma (3P)	Lognormal (2P)	Lognormal (3P)
24/11/2005	6	5	4	1	3	2
5/1/2006	6	5	4	1	3	2
22/1/2006	6	5	4	2	3	1
7/3/2006	6	5	4	2	3	1
9/10/2006	6	5	3	1	4	2
23/11/2006	6	5	3	2	4	1
11/2/2007	6	5	4	1	3	2
8/12/2007	6	5	4	2	3	1
2/4/2008	6	2	3	5	4	1
27/1/2009	6	5	3	2	4	1
6/4/2009	6	4	2	5	3	1
10/12/2009	6	2	4	5	3	1
28/1/2011	6	5	4	2	3	1
24/2/2011	6	5	4	2	3	1
19/12/2011	6	5	4	2	3	1
18/4/2012	6	5	4	1	3	2
18/5/2012	6	4	3	5	2	1
29/12/2012	6	5	4	2	3	1
Best fit	0	0	0	5	0	13
Percentage	0%	0%	0%	28%	0%	72%

Table 4. Best fit for convective events.

Event Date	Exponential (1P)	Exponential (2P)	Gamma (2P)	Gamma (3P)	Lognormal (2P)	Lognormal (3P)
11/17/2005	6	5	1	2	4	3
2/5/2006	6	5	4	1	2	3
9/23/2006	6	5	4	3	1	2
10/7/2006	6	5	3	2	4	1
5/19/2007	6	3	2	5	4	1
10/20/2007	6	3	4	5	2	1
12/8/2008	6	5	1	2	3	4
3/21/2009	6	5	1	2	3	4
2/8/2010	6	5	4	1	3	2
6/12/2011	6	5	4	2	3	1
12/21/2011	6	2	1	5	3	4
1/16/2013	6	5	3	2	4	1
1/25/2013	6	5	1	2	3	4
2/22/2013	6	5	1	2	3	4
11/11/2013	6	5	1	3	4	2
11/24/2013	6	5	4	1	3	2
1/24/2014	6	5	4	2	3	1
1/26/2014	6	5	4	2	3	1
Best fit	0	0	7	3	1	7
Percentage	0%	0%	39%	17%	6%	39%

As seen in Table 3, in the selected stratiform events the 3-P lognormal distribution is the best fit in 72% of the occasions. The 3-P gamma distribution is the best fit in the remaining 28% of the occasions. However, differences between the lognormal and gamma types of distributions regarding the K–S test statistic D_n, were marginal as the difference in the value of the test statistic was very small. The type of

distribution that has outperformed in relation with the other two, is exponential distribution, where both 1-P and 2-P exponential distributions, performed poorly in almost all occasions.

The main difference in Table 4, in comparison with Table 3, is that the results in convective events are diversified. Now, the 2-P gamma distribution is equally good fit with the 3-P lognormal distribution, scoring as a best fit both in 39% of the cases. In addition, the 3-P gamma distribution performed best in 16% of the cases, and 2-P lognormal distribution was the best fit in 6% of the cases. Similarly with the stratiform events, both 1-P and 2-P exponential distributions outperformed in comparison with lognormal and gamma distributions. Although it was expected that the lognormal distribution, which is a heavy tailed distribution, would have given better fitting in the convective events, this did not occur. One possible explanation is the fact that convective events have relatively more counts on the upper bins than stratiform ones, so theoretically more drops will surpass the diameter limitation of the JWD (5.373 mm) and will automatically be "truncated" by the instrument affecting the fitting results on the convective type in a greater extent than in the stratiform type of rainfall.

5. Conclusions

Thirty six rainfall events have been selected from a JWD database covering the period (2005–2014) and their respective DSDs have been studied for depicting the best fit among six statistical distributions. The selected distributions were 1-P and 2-P exponential, 2-P and 3-P lognormal and 2-P and 3-P gamma distributions. Rainfall events were classified according to the precipitation type: stratiform and convective. The criteria for rainfall event selection and categorization were the total rainfall accumulation and the rainfall duration. Distinct rainfall events were assumed for those which were separated with at least one-hour no-rain interval. The Kolmogorov–Smirnov test was implemented for the determination of the best fit of actual data to the theoretical distributions. The ranking criterion was the smallest test statistic D_n. Findings denote that as far as stratiform events are concerned, 3-P lognormal distribution was the best fit in 72% of the cases, while in the remaining 28% of the cases, 2-P gamma distribution was the best fit. On the contrary, in convective events, 2-P gamma distribution and 3-P lognormal distributions performed equally good, being the best fit both in 39% of the studied events. In addition, in 16% of the cases, 3-P gamma distribution was the best fit, and, in 6% of the cases, the best fit was 2-P lognormal distribution.

Acknowledgments: The constructive reviews of anonymous reviewers are warmly acknowledged.

Author Contributions: These authors contributed equally to this work.

Conflicts of Interest: The authors declare no conflict of interest.

References

1. Winder, P.; Paulson, K.S. The measurement of kinetic energy and rain intensity using an acoustic disdrometer. *Meas. Sci. Technol.* **2012**, *23*, 015801. [CrossRef]
2. Kruger, A.; Krajewski, W.F. Two-Dimensional Video Disdrometer: A Description. *J. Atmos. Oceanic Technol.* **2002**, *19*, 602–617. [CrossRef]
3. Schönhuber, M.; Lammer, G.; Randeu, W.L. The 2-D-Video-Distrometer. In *Precipitation: Advances in Measurement, Estimation and Prediction*; Springer: Berlin, German, 2008.
4. Joss, J.; Waldvogel, A. Ein spektrograph fur niederschlagstrophen mit automatischer auswertung. *Pure Appli. Geophys.* **1967**, *68*, 240–246. [CrossRef]
5. Ignaccolo, M.; De Michele, C. Phase space parameterization of rain: The inadequacy of gamma distribution. *J. Appl. Meteor. Clim.* **2014**, *53*, 548–562. [CrossRef]
6. Adirosi, E.; Baldini, L.; Lombardo, F.; Russo, F.; Napolitano, F.; Volpi, E.; Tokay, A. Comparison of different fittings of drop spectra for rainfall retrievals. *Adv. in W. Res.* **2015**, *83*, 55–67. [CrossRef]
7. Kottek, M.; Grieser, J.; Beck, C.; Rudolf, B.; Rubel, F. World map of the koppen-geiger climate classification updated. *Met. Zeitschrift* **2006**, *15*, 259–263. [CrossRef]

8. Hellenic National Meteorological Service. Available online: http://www.hnms.gr/hnms/greek/index_html (accessed on 6 February 2016).
9. Papathanasiou, C.; Makropoulos, C.; Baltas, E.; Mimikou, M. An innovative approach to floods and fire risk assessment and management: The flire project. In Procedings of the 8th International Conference of EWRA "Water Resources Management in an Interdisciplinary and Changing Context", Porto, Portugal, 26–29 June 2013.
10. Tokay, A.; Wolff, R.K.; Bashor, P.; Dursun, K.O. On the measurement errors of the joss-waldvogel disdrometer. In Procedings of the 31st International Conference on Radar Meteorology, Seattle, WA, USA, 6–12 August 2003.
11. Tokay, A.; Kruger, A.; Krajewski, W.F. Comparison of drop size distribution measurements by impact and optical disdrometers. *J. Appl. Meteorol.* **2001**, *40*, 2083–2097. [CrossRef]
12. Tokay, A.; Short, A.D. Evidence from tropical raindrop spectra of the origin of rain from stratiform *versus* convective clouds. *J. App. Met. Clim.* **1996**, *35*, 355–370. [CrossRef]
13. Bringi, V.N.; Williams, C.R.; Thurai, M.; May, P.T. Using dual-polarized radar and dual-frequency profiler for dsd characterization: A case study from darwin, australia. *J. Atm. Oc. Tech.* **2009**, *26*, 2107–2122. [CrossRef]
14. Caracciolo, C.; Prodi, F.; Battaglia, A.; Porcu, F. Analysis of the moments and parameters of a gamma dsd to infer precipitation properties: A convective stratiform discrimination algorithm. *Atm. Res.* **2006**, *80*, 165–186. [CrossRef]
15. Ricciardulli, L.; Prashant, D.S. Local time and space scales of organized tropical deep convection. *J. Clim.* **2002**, *15*, 2775–2790. [CrossRef]
16. Mathwave, T. Easyfit, 5.6 Professional. Available online: http://www.mathwave.com/company.html (accessed on 6 February 2016).
17. Marshall, J.S.; Palmer, W.M. The distribution of raindrops with size. *J. Meteor.* **1948**, *5*, 165–166. [CrossRef]
18. Ulbrich, W.C. Natural variations in the analytical form of the raindrop size distribution. *J. Clim. Appl. Meteorol.* **1983**, *22*, 1764–1775. [CrossRef]
19. Feingold, G.; Levin, Z. The lognormal fit to raindrop spectra from convective clouds in israel. *J. Clim. Appl. Meteorol.* **1986**, *25*, 1346–1363. [CrossRef]
20. Kliche, V.D.; Smith, L.P.; Johnson, W.R. L-moment estimators as applied to gamma drop size distributions. *J. Appl. Meteorol. Clim.* **2008**, *47*, 3117–3130. [CrossRef]
21. Cao, Q.; Zhang, G. Errors in estimating raindrop size distribution parameters employing disdrometer and simulated raindrop spectra. *J. Appl. Meteorol. Clim.* **2009**, *48*, 406–425. [CrossRef]